Breakup of a multisoliton state of the linearly damped nonlinear Schrödinger equation

Jaroslaw E. Prilepsky
B.I. Verkin Institute for Low Temperature Physics and Engineering, 47 Lenin Avenue, Kharkov 61103, Ukraine

Stanislav A. Derevyanko*
Photonics Research Group, Aston University, Aston Triangle, Birmingham B4 7ET, United Kingdom
(Received 8 November 2006; published 28 March 2007)

We address the breakup (splitting) of multisoliton solutions of the nonlinear Schrödinger equation (NLSE), occurring due to linear loss. Two different approaches are used for the study of the splitting process. The first one is based on the direct numerical solution of the linearly damped NLSE and the subsequent analysis of the eigenvalue drift for the associated Zakharov-Shabat spectral problem. The second one involves the multisoliton adiabatic perturbation theory applied for studying the evolution of the solution parameters, with the linear loss taken as a small perturbation. We demonstrate that in the case of strong nonadiabatic loss the evolution of the Zakharov-Shabat eigenvalues can be quite nontrivial. We also demonstrate that the multisoliton breakup can be correctly described within the framework of the adiabatic perturbation theory and can take place even due to small linear loss. Eventually we elucidate the occurrence of the splitting and its dependence on the phase mismatch between the solitons forming a two-soliton bound state.

DOI: 10.1103/PhysRevE.75.036616 PACS number(s): 42.81.Dp

I. INTRODUCTION

The stability of higher-order soliton solutions propagating in weakly dispersive Kerr media under the action of various perturbations has been intensively studied in various contexts over the last few decades. Such models have a multitude of physical applications, from hydrodynamics and plasma physics to nonlinear fiber optics [1,2]. Soliton propagation is modeled by the nonlinear Schrödinger equation (NLSE) with the nonzero right-hand side (RHS) corresponding to a perturbation. In the absence of a perturbation the NLSE is integrable by the inverse scattering transform (IST) technique [3,4]. The decomposition of the NLSE solution based on the IST method (the direct spectral transform) allows one to separate the solution of the unperturbed NLSE into a combination of a soliton part, determined solely by the discrete eigenvalues of the associated Zakharov-Shabat spectral problem (ZSSP), and background radiation determined by the continuous spectrum of the same eigenproblem. Of particular interest are the N-soliton solutions corresponding to a ZSSP with no continuous spectrum and $N \geq 2$ discrete eigenvalues, $\zeta_n = \xi_n + i\eta_n$, located at the upper complex half-plane of the ZSSP spectral parameter ζ. Each discrete eigenvalue corresponds to an individual soliton with the real part ξ_n providing the soliton velocity and imaginary part η_n determining the soliton amplitude (both up to the factor of 2). In the unperturbed case the discrete eigenvalues are integrals of motion and the evolution of the other parameters, such as soliton phase and position, can be inferred from the evolution of the so-called Jost coefficients [3,4]. A special class of N-soliton states ($N \geq 2$) is defined by purely imaginary eigenvalues of the associated ZSSP, when all the velocities ξ_n are exactly equal to zero. Then the system is said to be in a *bound state* and emerging solutions are often called *breathers*. Such solutions undergo periodic oscillations in shape during the propagation with individual solitons remaining localized so that the solution remains stable. The period of such oscillations is determined by the values of imaginary eigenvalues η_k. It is necessary to note that these bound states of N solitons are not strictly bound in the traditional sense since their binding energy is exactly zero [4]. An important consequence of that is that if one adds a perturbation to the original integrable NLSE, a breather is likely to become unstable and break up into dispersing individual solitons.

The breather instability has been investigated extensively for various types of perturbations. The effect of linear loss on a NLSE breather was studied both analytically and numerically in [5–9]. In the first two references the stability of the two-soliton breather was inferred provided that loss is adiabatically small. As we shall see from the current study this is not exactly the case: for a given value of loss a breather can be both stable and unstable depending on the initial parameters, in particular the initial phase mismatch between the solitons. In the context of nonlinear fiber optics the multisoliton splitting was observed for perturbations corresponding to intrapulse Raman scattering, self-steepening, and third-order dispersion [10–13]. The splitting of bound spatial multisoliton states was also shown to occur due to two-photon absorption [14], soliton reflection at a material interface [15], soliton interaction with a periodic optical lattice [16], and refractive index variation [17]. The effects of higher-order nonlinearities have also been considered [18]. A great deal of attention has been dedicated to the behavior of the multisoliton states in the presence of linear filtering and/or linear gain [19–22]. The combined action of dissipative filtering and linear loss was considered in [23] (see also [5]).

In the current work we study the splitting of bound states by linear loss only. For the case of two bound solitons such a splitting was predicted in [8] but it was attributed to the strong nonadiabatic nature of linear loss. In [6] the effect of small linear loss was analyzed via adiabatic perturbation

*On leave from Institute for Radiophysics and Electronics, Kharkov, Ukraine. Electronic address: s.derevyanko@aston.ac.uk

theory and it was concluded that the breather remains stable (which seemingly concurs with early numerical results of [5]). In Ref. [23] it was predicted that the splitting of bound soliton states occurs via the intermediate eigenvalue coalescence but it was stated that the effect only takes place if one adds dissipative filtering perturbation to the linear loss.

The purpose of the current paper is twofold. First, we wish to clarify the issue of whether linear loss (large or small) acting alone can split a bound soliton state. We demonstrate that not only is it sufficient to have just a linear loss to produce soliton splitting but also that such a splitting can be adequately described by means of adiabatical perturbation theory in the case of small loss for two bound solitons (this result differs from that of Ref. [6]), and this statement is also supported by direct numerical simulations of the soliton dynamics. The splitting, however, does not occur for all possible values of the initial parameters, and we demonstrate numerically that the splitting effect is sensitive to the initial phase mismatch between the individual solitons.

The second goal of the paper is to describe the complicated dynamics and mutual interaction of complex eigenvalues of the ZSSP for a higher number of bound soliton states, $N>2$, in the case of strong loss. We demonstrate that during the (nonadiabatic) evolution of a multisoliton pulse the eigenvalues not only bifurcate causing the pulse to break up but also individual eigenvalues can disappear and reemerge during the evolution due to complex variations in the pulse shape. The latter effects have clearly nonadiabatic nature and are only observed for strong loss and a large number of solitons.

In both adiabatic and nonadiabatic regimes, as one would expect in purely dissipative systems, the imaginary parts of the eigenvalues (related to the soliton amplitudes) and hence the power content of the pulse (or density of quasiparticles) on average decrease exponentially with the propagation. Also in both cases of large and small loss the splitting occurs when the initially bound (i.e., imaginary) eigenvalues attract each other and eventually coalesce (an effect similar to that discussed in [23]), after which the two eigenvalues acquire nonzero real parts (i.e., the individual solitons acquire velocities). These velocities are always equal in magnitude and have opposite signs provided that the initial pulse shape is an even function so that the momentum of the pulse is zero.

During our analysis we used two different approaches concurrently. In the first one, which we call the *direct spectral propagation method*, we used a combination of the second order split-step Fourier method to propagate the pulse [1] and the numerical analysis of the ZSSP spectrum [24] to analyze the evolution of the soliton content of the pulse. It is worth mentioning that a similar method relying on the concurrent use of direct numerical integration of the NLSE and ZSSP field decomposition was first suggested in Ref. [25]. The advantage of this method is that it does not rely on the IST to propagate the solution and hence can be used for the systems far from integrable, when the loss cannot be accounted for perturbatively. The disadvantage of this method is that it is quite expensive computationally since the numerical resolution of close ZSSP eigenvalues with the desired accuracy imposes a significant CPU time overhead. The second method relies on adiabatic perturbation theory for the ZSSP eigenvalues [26]. In this method we use the exact Jost functions for a two-soliton state (with nonzero velocities) [22] rather than the approximate quasiparticle methods of [27] applicable only when the solitons are well separated. The reason for such a choice (which makes the analysis somewhat more complicated compared to the quasiparticle method) is that the sought soliton splitting occurs due to the strong nonlinear interaction of the individual solitons which only takes place when the latter overlap strongly. The advantage of the adiabatic perturbation theory compared to the direct spectral propagation method is that the system of equations is now much simpler, and for the case of $N=2$ bound solitons it is possible to write down the unperturbed Jost functions in a closed analytical form (see the Appendix). The drawback of the adiabatic perturbation theory, however, is that it is only applicable for systems close to integrable (small loss) and does not account for the effects of the radiative part of the solution. In the present paper we compare and discuss the results of the two approaches.

II. DYNAMICS OF ZSSP EIGENVALUES: DIRECT SIMULATION OF STRONGLY DAMPED BREATHERS

We start with the linearly damped NLSE

$$\frac{\partial q}{\partial z} - \frac{i}{2}\frac{\partial^2 q}{\partial t^2} - i|q|^2 q + \frac{\alpha}{2} q = 0. \tag{1}$$

This equation has wide area of application. For instance, in the context of nonlinear fiber optics Eq. (1) describes (in normalized units) the propagation of the optical pulse envelope in a silica fiber with the linear loss coefficient α [1]. In the absence of loss, $\alpha=0$, Eq. (1) is integrable by the IST technique [3,4]. In this approach Eq. (1) is recast as a compatibility condition between two sets of linear equations, one of which forms the following spectral problem (ZSSP):

$$i\frac{\partial \psi_1}{\partial t} + q\psi_2 = \zeta\psi_1,$$

$$-q^*\psi_1 - i\frac{\partial \psi_2}{\partial t} = \zeta\psi_2. \tag{2}$$

The other set of equations describes the z evolution of the Jost functions $\psi_{1,2}(t,z)$. It turns out that the complete information about the solution of NLSE is contained in a set of *scattering data* defined as

$$r(\xi) = b(\xi)/a(\xi) \quad \text{for real } \xi,$$

$$\zeta_n \quad \text{and} \quad C_n = \left.\frac{b(\zeta)}{a'(\zeta)}\right|_{\zeta=\zeta_n}, \quad n = 1, \ldots, N. \tag{3}$$

Here $a(\zeta)$ and $b(\zeta)$ are the first and second Jost coefficients (see [3,4]) and the quantities ζ_n represent the discrete ZSSP spectrum of Eqs. (2) and are given by the equation $a(\zeta_n)=0$. The important feature of IST is that the z evolution of the scattering data is trivial:

$$\frac{d\zeta_n}{dz} = 0, \tag{4a}$$

$$C_n(z) = C_n(0)e^{2i\xi_n^2 z}, \tag{4b}$$

$$r(\xi,z) = r(\xi,0)e^{2i\xi^2 z}. \tag{4c}$$

Given spectral data (4) the solution $q(z,t)$ can be obtained by solving an inverse scattering problem which involves solving a linear system of integral equations—a Gel'fand-Levitan-Marchenko system [3,4].

An important class of solutions of the unperturbed NLSE is the N-soliton solutions corresponding to the reflectionless potentials $q(0,t)$ for which $r(\xi,0)=0$. Such solutions are described in the Appendix where we provide the general analytical form for the Jost functions $\psi_{1,2}$ and the solution $q(z,t)$ for the case $N=2$. The physical meaning of the scattering data is the following. The discrete eigenvalues $\zeta_n=\xi_n+i\eta_n$ determine the velocity and amplitude of each soliton (up to a factor of 2) while the complex coefficients $C_n(0)$ are related to the initial position and phase. In particular, if all the soliton velocities ξ_n are zero, such a solution is said to form a bound state or a *breather*. A breather is a collection of N overlapping solitons that always remain localized in t while experiencing periodic beating in z. The period of beating between each pair of solitons is given by

$$Z_{ij} = \frac{\pi}{|\eta_i^2 - \eta_j^2|}. \tag{5}$$

One particular form of N-soliton solution was considered by Satsuma and Yajima [28] and arises from the following input pulseform: $q(0,t)=N\,\mathrm{sech}\,t$. Its discrete imaginary ZSSP eigenvalues are $\zeta_n=i(N-n+1/2)$, $n=1,\ldots,N$, and the overall period of z oscillations is given by the lowest common beat frequency: $Z_p=\pi/2$.

The IST method described above is only applicable to the unperturbed NLSE, when $\alpha=0$. The question then arises as to what happens to a breather when one includes a dissipative perturbation. It is known that if the perturbation is small, the system remains close to integrable and one can use adiabatic perturbation theory [26] to describe slow variations of the scattering data and hence the parameters of individual solitons. This approach will be applied in the next section. Here, however, we would like to consider a more general case when the evolution is nonadiabatic and the system is far from integrable so that perturbative approach fails. What is the criterion for the loss to be nonperturbative? One is tempted to compare the $1/e$ attenuation length $Z_a=1/\alpha$ with the common beating period of the unperturbed breather, Z_p, so that $\alpha Z_p \gtrsim 1$ will correspond to a nonperturbative regime (or strong loss). However, this criterion is meaningless since the parameters of the breather evolve simultaneously with z and so do the beat periods (5) which makes any estimate based on the initial values of breather parameters rather unreliable. Moreover, as we shall see in Sec. III the very form of the solution can change drastically when a breather splits and z evolution of the pulse becomes aperiodic so that $Z_p \to \infty$. However, this phenomenon can still be adequately described within the framework of perturbation theory. Therefore the genuine applicability criterion for a perturbative treatment is different, and indeed as was shown by Blow and Doran [7] the $1/e$ attenuation length should be compared simply to the maximum propagation distance z_{max}. If $\alpha z_{max} \ll 1$, the dynamics of the eigenvalues is smooth and adiabatic so that the perturbative approach works well; otherwise, perturbation theory fails and the systems evolves nonadiabatically for all z such that $\alpha z \gtrsim 1$. One important conclusion is that however small the loss coefficient α is, the system will eventually enter the nonadiabatic stage given that we propagate the solution long enough. This section concentrates on the case of nonadiabatic evolution of a breather.

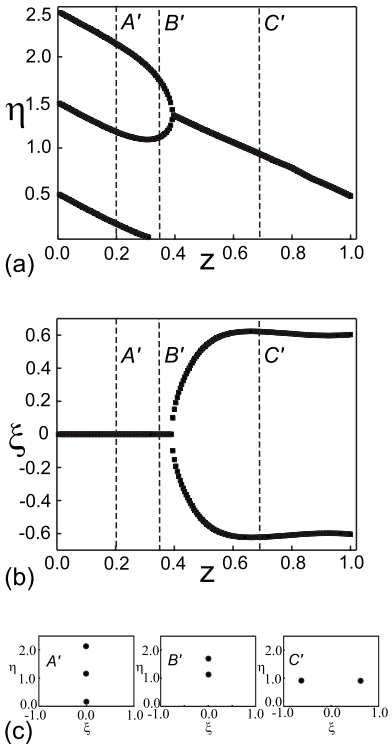

FIG. 1. The dynamics of real (a) and imaginary (b) parts of the ZSSP eigenvalues for the initial pulse $q(0,t)=3\,\mathrm{sech}(t)$. The bottom part of the figure [(c)] gives the locations of the discrete complex eigenvalues (ξ_n,η_n) for three different slices in z labeled A', B', and C' in panels (a) and (b).

Inasmuch as no analytical tool is available for the nonadiabatic regime, one needs to resort to numerical analysis to study the the details of breather dynamics and stability. We suggest the following numerical scheme. We employ a second-order split-step Fourier method [1] to solve Eq. (1) and propagate the initial pulse. At the same time at a set of given points in z we use the numerical procedure given in [24] to analyze the spectral content of ZSSP, Eq. (2). This will enable us to track the dynamics of the discrete eigenvalues of ZSSP and hence the parameters of each individual soliton. For the initial form of an N-soliton solution we pick that of Satsuma and Yadjima with $N=3$ and $N=5$. The results of our numerical simulations are presented in Figs. 1 and 2. One can see that the higher the number of solitons, the more complicated is the dynamics. In both cases the attenuation was chosen to be $\alpha=1.15$, while the maximum distance was $z_{max}=1$ so that the product αz_{max} was close to unity during the most part of evolution. Let us start from the three-soliton

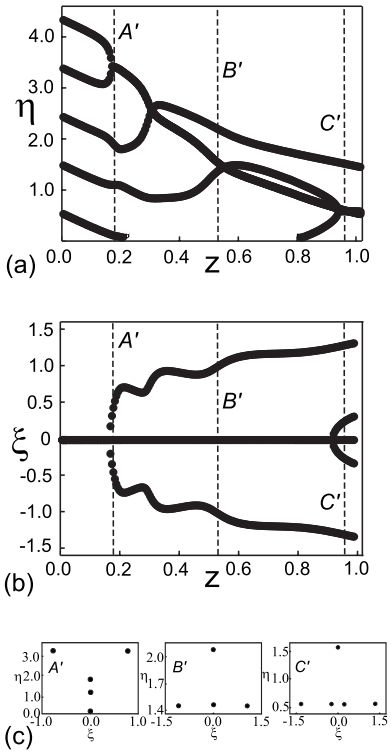

FIG. 2. The dynamics of real (a) and imaginary (b) parts of the ZSSP eigenvalues for the initial pulse $q(0,t)=5\ \mathrm{sech}(t)$. The bottom part of the figure [(c)] gives the locations of the discrete complex eigenvalues (ξ_n, η_n) for three different slices in z labeled A', B', and C' in panels (a) and (b).

case in Fig. 1. The breakup of the breather is manifested as a symmetric bifurcation in the z dependence of the real parts of two solitons, Fig. 1(a), occurring at $z \approx 0.39$. The imaginary parts of those two solitons coalesce at the same point [see Fig. 1(b)] and continue to decay simultaneously. The symmetric form of the bifurcation and the equality of the imaginary parts after the coalescence are in agreement with the fact that the momentum of the initial pulse is exactly zero. Indeed, the momentum of the pulse is defined as

$$M = \mathrm{Im} \int_{-\infty}^{\infty} (\partial q/\partial t) q^* \, dt. \tag{6}$$

From Eq. (1) it follows that the momentum evolves with z as $M(z)=M(0)\exp[-\alpha z]$. Since the initial pulse form $q(0,t)=N\ \mathrm{sech}\ t$ is an even function of t, the momentum $M(z)$ will always remain zero. On the other hand, it is known [4] that the momentum of the N-soliton solution can be expressed in terms of the discrete eigenvalues as $M=-(1/2)\Sigma_{i=1}^{N} \xi_i \eta_i$. Therefore a symmetric bifurcation of the pairs of eigenvalues, $\zeta_1=\xi+i\eta$, $\zeta_2=-\xi+i\eta$, preserves zero total momentum.

Another visible effect is the disappearance of the lowest (third) eigenvalue at $z \approx 0.35$. The question of whether a soliton can be actually destroyed by linear loss is a difficult one. It is known that the effects of creation and annihilation of solitons can only occur in the nonadiabatic regime when the changes of the eigenvalues are quite drastic. In fact, what we can confirm is that the imaginary part of an eigenvalue falls below the accuracy threshold of our numerical ZSSP analyzer (which is at the level of 10^{-3}). In practical terms this means that regardless of whether a bound state remains finite or not its impact on the dynamics of the other states and pulse content below the threshold is negligible. Therefore we will refer to this effect as a soliton annihilation.

The remaining two bifurcated eigenvalues continue to drift simultaneously with the imaginary parts decreasing due to loss. The real parts (i.e., velocities) eventually stabilize which is due to the fact that at this stage of the evolution the individual soliton pulses are well separated and only affect each other via small exponential tails.

When the initial number of bound soliton states increases the dynamics of the eigenvalues becomes ever more complicated. The dynamics of $N=5$ soliton states is given in Fig. 2. The mutual interaction of the eigenvalues leads to multiple bifurcations as well as to soliton creation-annihilation. At the first stage of the evolution [see slice A' in Figs. 2(a)–2(c)] we observe that the highest two eigenvalues have bifurcated while the lowest one is about to disappear. Between the stages A' and B' the lowest eigenvalue disappears completely while the pair of symmetric bifurcated eigenvalues slowly approaches the real axis. Note, however, that the dynamics of the remaining purely imaginary eigenvalues is not monotonic. Due to mutual interaction (as well as the influence of the bifurcated symmetric pair), their magnitude initially increases. Between the stages B' and C' we observe the reappearance of the fifth eigenvalue at $z \approx 0.8$. This reemerged eigenvalue is attracted to the lowest of the remaining two imaginary eigenvalues which eventually leads to their coalescence and the appearance of a second bifurcation.

The multitude of dynamical effects observed in the perturbed ZSSP is not restricted to the effects described above. In fact, for the Gaussian shape of the initial pulse we were able to observe the effect which is opposite to the bifurcation—i.e., the reverse coalescence of the initially bifurcated soliton states due to interaction with yet another bound state. True, the Gaussian pulse shape is not an exact N-soliton solution of the NLSE but it quickly evolves into such during the propagation. The conversion of a Gaussian pulse to a multisoliton solution in a lossy NLSE is a subject of a different study that will be published elsewhere.

From the results presented above one might conclude that the eigenvalue bifurcations and breather splitting occur always given that the product αz_{max} is much larger or the same order as unity. This is not the case, however. Hasegawa and Nyu [9] (see also Chap. 4 in [2]) also considered the eigenvalue dynamics of a linearly damped three-soliton Satsuma-Yajima breather (similar to that shown in Fig. 1). However, their choice of parameters corresponds in our notation to $\alpha=11.04$ and $z_{max}=0.1$. For such values of the parameters they found that the lowest eigenvalue disappears (similar to the situation in Fig. 1) but the remaining two do not bifurcate and stay on the imaginary axis so that the breather is still stable. Our own simulations confirm their result. For $z=0.1$ our simulation gives the following values of the remaining eigenvalues: $\eta_1=0.235$ and $\eta_2=1.220$, with the real parts equal to zero up to the computational accuracy of the method. This is in a good agreement with the results of Hasegawa and Nyu (see Fig. 4.6 of [2], noting that the scale is

logarithmic and their definition of η differs from ours by the factor of 2). As in the case shown in our Fig. 1 the product αz_{max} is close unity. This signals that the effect of splitting depends not solely on the product αz but rather on the values of both loss and propagation distance separately.

Given the complicated eigenvalue dynamics described in this section one might also wonder whether the effects of soliton splitting (eigenvalue bifurcations) can be observed only for strong loss (as initially suggested in [8]) and how one can study and quantify such a phenomenon in more detail. In the next section we demonstrate that such a splitting may occur even for small values of loss in a two-soliton bound state and can be adequately described by means of the two-soliton adiabatic perturbation theory.

III. ADIABATIC EVOLUTION OF ZSSP DATA

When studying the effects of mutual interaction between the solitons in the presence of small linear loss it is customary to use the most simple single-soliton variant of the perturbation theory [27]. Such a choice is well justified when the solitons are well separated from each other so that the overlapping between the solitons is small and the whole multisoliton solution can be approximated by a linear combination of separate single solitons. However, this simplest version of the perturbation theory cannot be applied if one wants to study the possibility of breather splitting. Indeed such a splitting occurs as a consequence of strong nonlinear interaction of individual solitons when the pulse overlapping is essential and one simply cannot use single-soliton perturbation theory. Because of that, one has to resort to the multisoliton perturbation theory for the scattering data of the N-soliton solution. The general form of the equations determining the adiabatic evolution of the spectral data is [22,26]

$$i\frac{d\zeta_n}{dz} = -\frac{1}{D_n(a_n')^2}\int_{-\infty}^{\infty}(R^*\psi_{1,n}^2 - R\psi_{2,n}^2)dt, \tag{7}$$

$$i\frac{dD_n}{dz} = 2\zeta_n^2 D_n + \frac{a_n''}{(a_n')^3}\int_{-\infty}^{\infty}\left(R^*\psi_{1,n}^2 - R\psi_{2,n}^2\right)dt - \frac{1}{(a_n')^2}\int_{-\infty}^{\infty}\left(R^*\frac{\partial\psi_1^2}{\partial\zeta} - R\frac{\partial\psi_2^2}{\partial\zeta}\right)\Bigg|_{\zeta_n} dt. \tag{8}$$

Here for the sake of convenience we introduced another quantity $D_n=(b_n a_n')^{-1}=C_n^{-1}(a_n')^{-2}$ instead of C_n [22]. On the RHS of both equations R is a perturbation term, which in our case of linear loss is $R=-\alpha q(z,t)/2$. The Jost functions and the perturbation R entering Eqs. (7) and (8) are all functions of ζ_n and D_n (see the Appendix), so that we arrive at a system of $2N$ coupled nonlinear equations, N being the number of bound solitons. These equations do not account for the effects of the linear radiation (these effects are of the higher order of the perturbation theory). As mentioned in the previous section the applicability condition for the adiabatic perturbation theory, Eqs. (7) and (8), is $\alpha z_{max} \ll 1$, where z_{max} is the maximum propagation distance. In the absence of perturbation ($\alpha=0$) one naturally recovers the unperturbed evolution of the spectral parameters, Eqs. (4a) and (4b), from Eqs. (7) and (8). The calculation of the derivatives of Jost function with respect to ζ in the second integrand of Eq. (8) can be simplified by expressing these via the Jost functions themselves [22].

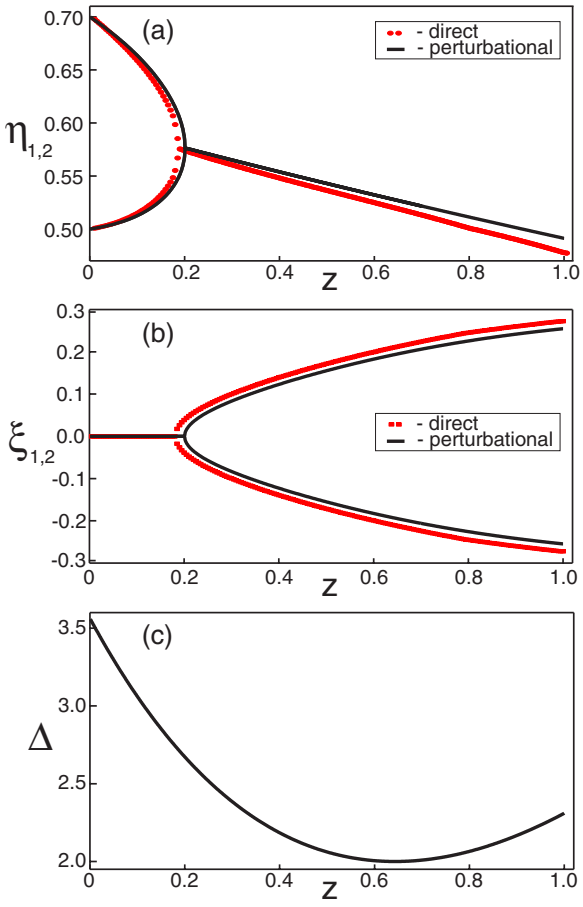

FIG. 3. (Color online) Comparative plots of the ZSSP eigenvalue dynamics for a two-soliton breather. The loss coefficient $\alpha=0.2$, the initial breather amplitudes $\eta_1=0.5$ and $\eta_2=0.7$, and the initial phase mismatch is $\delta\sigma_{12}=-0.3$. The other characteristics of the initial breather profile are $\xi_{1,2}=0$ and $\vartheta_{1,2}^0=0$. For the definition of breather parameters see the Appendix. (a) The dynamics of η_n, $n=1,2$, inferred from the integration of the perturbation theory equations (7) and (8) (solid line) and direct spectral propagation method (circles). (b) The dynamics of ξ_n, $n=1,2$, obtained via the perturbation theory (solid line) and direct method (squares). The panel (c) illustrates the variation of the quantity Δ, Eq. (A6), taken at $t=0$ and characterizing the oscillations of the shape of a breather.

In order to proceed with the perturbation theory one needs to know the explicit form of the Jost functions $\psi_{1,2}$. As shown in [3,4] these can be obtained as solutions of a certain system of linear algebraic equation; see Eqs. (A2) in the Appendix. However, the compact explicit expressions for the Jost functions are available only for the case $N=2$ [see Eqs. (A9) and (A10)], so in this section we will restrict our treatment to two-soliton bound states only. In Figs. 3 and 4 we show the dynamics of the ZSSP eigenvalues during the propagation of a two-soliton breather inferred from the perturbation theory equations and superimpose the same dynamics obtained via the direct spectral propagation method of

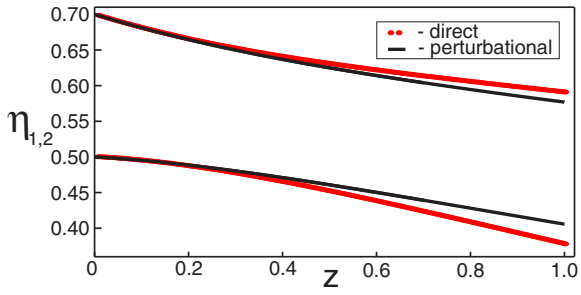

FIG. 4. (Color online) The same as in Fig. 3(a), but with the initial phase mismatch between the two components of a breather set to $\delta\sigma_{12}=0.4$.

Sec. II. The general form of an unperturbed 2-soliton solution is given by formula (A11). If the velocities $\xi_{1,2}$ are equal to zero, we have a two-soliton breather. The periodic beating between the individual components of the breather causes the pulses to overlap strongly which occurs when the quantity Δ, Eq. (A6), taken at the origin $t=0$ reaches its minimum. When analyzing the dynamics of individual eigenvalues (Fig. 3) it is useful to introduce the initial phase mismatch between the solitons defined as $\delta\sigma_{12}=\sigma_1^0-\sigma_2^0-\pi$, where $\sigma_{1,2}^0$ are the initial phases of the solitons appearing in Eq. (A8). The choice of $\delta\sigma_{12}=0$ corresponds to the initially overlapping pulses. In Fig. 3 the initial phase mismatch parameter is negative, $\delta\sigma_{12}=-0.3$, which (given that $\eta_1<\eta_2$) indicates that we start the evolution before the overlapping point. When a small loss is included the position of the overlapping point changes compared to that of the unperturbed breather due to adiabatically slow change of the soliton parameters.

From Fig. 3 it is obvious that the breather breakup can take place solely due to the effect of small linear loss, and this process can be described within the framework of adiabatic perturbation theory. The imaginary ZSSP eigenvalues attract each other and then collide at the breakup point Z_b, acquiring symmetric real parts. The collision of the imaginary eigenvalues and the appearance of the real parts have bifurcational behavior completely analogous to that observed in the dynamics of multisoliton breathers in the nonadiabatic regime (see Figs. 1 and 2). One also notes that the data obtained with two different methods agree nicely. This indicates that the perturbation theory does describe the process of the two-soliton splitting adequately. The perturbative analysis can yield the position of the bifurcation point, Z_b, when the breather splitting occurs. As seen from the comparison between Figs. 3(a) and 3(b) and Fig. 3(c), the breakup point Z_b differs from the overlapping point of the two-soliton breather ansatz, defined by the minimum of the quantity Δ. For the initial set of parameters used in the simulation (see the caption of Fig. 3) the overlap point was $z\approx 0.62$, whereas the breakup occurred at $z\approx 0.2$, so that the minimum of Δ was at the point where the bound state had already broken up. After the coalescence of the eigenvalues and the subsequent bifurcation the perturbation theory remains valid as well, as indicated by the coincidence of the trajectories obtained by virtue of the two methods after the breakup point.

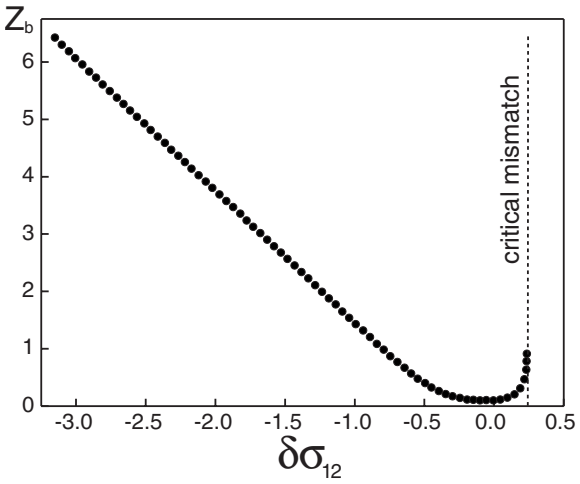

FIG. 5. The dependence of the breakup point Z_b on the value of the phase mismatch parameter $\delta\sigma_{12}$, inferred from Eqs. (7) and (8). The initial breather amplitudes $\eta_1=0.5$ and $\eta_2=0.7$, and the loss coefficient $\alpha=0.2$. The other characteristics of the initial breather profile are the same as in Fig. 3. The critical value of phase mismatch, $\delta\sigma_{12}\approx 0.296$, is depicted by the vertical dashed line.

One must also mention a strong dependence of the splitting on the phase mismatch value. For the next simulation run, depicted in Fig. 4, we used the same initial parameters as in Fig. 3 except for the phase mismatch, which was positive, $\delta\sigma_{12}=0.4$. As one can see, the eigenvalues in this case did not collide and eventually repelled one another, remaining purely imaginary, so that the coalescence did not occur and the breather remained stable. Again one observes a good agreement between the results of two methods with the small discrepancy due to nonadiabatic effects occurring as z approaches unity.

In Fig. 5 we show the dependence of the breakup point Z_b on the value of the initial phase mismatch for the breather with the initial values $\eta_1=0.5$ and $\eta_2=0.7$. We found that there exists a critical value of the mismatch, beyond which the solution remains stable during the whole evolution. Note that for positive $\delta\sigma_{12}$ the overlap point defined by the minimum of Δ lies beyond the propagation distance $z_{max}=1$. For our choice of η_1 and η_2 this critical point of the phase mismatch was approximately at $\delta\sigma_{12}\approx 0.296$. The value of Z_b sharply increases when approaching this point from below but remains finite. In the negative region of $\delta\sigma_{12}$ the breakup point Z_b grows monotonically, quickly approaching an almost linear dependence. It is worth mentioning that when one interchanges the initial values of η_1 and η_2, the picture in Fig. 5 is inverted with respect to the line $\delta\sigma_{12}=0$. Finally it is also worth noting that such a strong phase sensitivity of the eigenvalue dynamics resembles in a way a strong phase sensitivity of the interaction of two well-separated solitons in a lossless case [27].

Another instructive way of presenting the dynamical evolution of breather eigenvalues is by projecting the phase trajectories of Eqs. (7) and (8) onto the plane (η_1,η_2). In Fig. 6 we present the projections of several phase trajectories for the initial phase mismatch $\delta\sigma_{12}=-0.3$. The trajectories inside the upper triangle $(\eta_2>\eta_1)$ approach the bisector (the locus

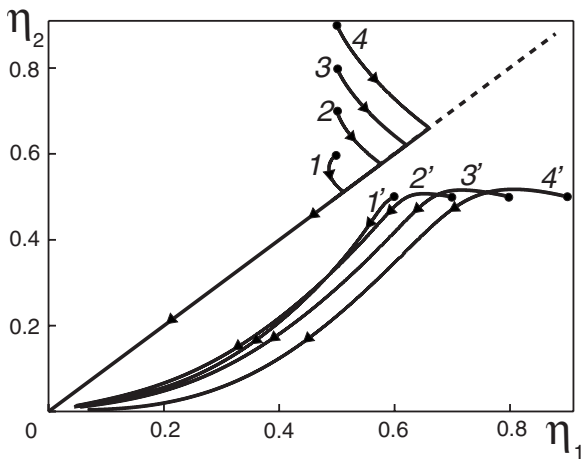

FIG. 6. The eigenvalue dynamics in the space of variables (η_1, η_2) obtained by numerical integration of Eqs. (7) and (8) for several values of the initial parameters η_1 and η_2. The initial phase mismatch was $\delta\sigma_{12}=-0.3$, the loss coefficient $\alpha=0.2$. The digits mark the trajectories with the following initial choices: 1: $\eta_1=0.5$, $\eta_2=0.6$. 2: $\eta_1=0.5$, $\eta_2=0.7$. 3: $\eta_1=0.5$, $\eta_2=0.8$. 4: $\eta_1=0.5$, $\eta_2=0.9$. The primed digits mark the trajectories with the values of η_1 and η_2 interchanged.

of the bifurcation points) and then evolve exponentially slowly towards the origin. The trajectories inside the lower triangle, $\eta_2 < \eta_1$, correspond to repelling eigenvalues. Such trajectories do not reach the bisector for the negative value of the mismatch chosen, $\delta\sigma_{12}=-0.3$, so that the solution remains stable and the eigenvalue coalescence does not occur. These trajectories still approach the origin exponentially due to the loss-stipulated decay of the soliton amplitudes. Such a behavior is easy to explain. As mentioned above the inversion of the phase portrait with respect to the bisector, $(\eta_1, \eta_2) \to (\eta_2, \eta_1)$, is equivalent to the inversion of the phase mismatch $\delta\sigma_{12} \to -\delta\sigma_{12}$. As we saw from Fig. 5 there exists a positive value of the phase mismatch above which the eigenvalue coalescence does not occur. Apparently this critical value is a function of the initial point in the space (η_1, η_2). The fact that the initial points 1–4 in the upper triangles in Fig. 6 do coalesce while their symmetric counterparts $1'-4'$ do not indicates that the critical values of phase mismatch for all points 1–4 do not exceed the absolute value of the chosen $\delta\sigma_{12}$, which is 0.3. The problem of determining the basins of attraction in the plane (η_1, η_2) and how these basins depend of the value of $\delta\sigma_{12}$ remains an open one and is not addressed in our study.

IV. CONCLUSION

In the present paper we have demonstrated that the breakup of a NLSE breather can occur through the action of linear loss only. The breakup manifests itself as a coalescence of discrete eigenvalues of the ZSSP with their subsequent bifurcational splitting and the appearance of symmetric nonzero velocities of individual solitons. This effect is adequately described by the adiabatic perturbation theory (for $N=2$ solitons) when the propagation length z_{max} is much less than the $1/e$ attenuation length. The breather splitting was also shown to be quite sensitive to the initial phase difference between the individual solitons: tuning the parameter $\delta\sigma_{12}$ one controls the breakup distance Z_b and can eventually stabilize the breather solution.

ACKNOWLEDGMENTS

We would like to thank Keith Blow for valuable comments and Sergei Turitsyn and Alexander Kovalev for interest in our work. This research was supported by the EPSRC.

APPENDIX: THE STRUCTURE OF THE *N*-SOLITON SOLUTION OF THE NLSE

For the exact N-soliton solution of the NLSE the reflection coefficient $r(\xi)$ vanishes at the real axis and the Jost coefficient $a(\zeta)$ becomes [3,4]

$$a(\zeta) = \prod_{n=1}^{N} \frac{\zeta - \zeta_n}{\zeta - \zeta_n^*}. \tag{A1}$$

Coefficients $C_n = b_n / a'(\zeta_n)$ evolve according to formula (4b). When the reflection coefficient vanishes the Gelfand-Levitan-Marchenko system of equations becomes a system of ordinary algebraic equations [3,4] for the set of Jost functions $\psi_l(\zeta_n)$. It is quite convenient to write this system in a matrix form. First we introduce the vectors $\mathbf{\Psi}_l = (\psi_l(\zeta_n), \ldots, \psi_l(\zeta_n))^T$ where $\psi_l(\zeta)$ are the components of the Jost functions. Then the desired system of equations reads

$$(\boldsymbol{I} + \boldsymbol{M}\boldsymbol{M}^*)\mathbf{\Psi}_2 = \boldsymbol{E}, \quad \mathbf{\Psi}_1 = \boldsymbol{M}\mathbf{\Psi}_2^*, \tag{A2}$$

where $\boldsymbol{I}$ is $N \times N$ identity matrix and $\boldsymbol{M}$ is $N \times N$ matrix with the elements $M_{mn} = e_m e_n^* C_n^* / (\zeta_n^* - \zeta_m)$ with $e_n = \exp(i\zeta_n t)$, the elements of the column vector $\boldsymbol{E} = (e_1, \ldots, e_N)^T$. The N-soliton solution of the NLSE can then be presented as

$$q(z,t) = -2\sum_{n=1}^{N} e_n^* C_n^* \psi_2^*(\zeta_n). \tag{A3}$$

For the reference let us write down the explicit form of the solution of Eqs. (A2) in the case of two bound states $N=2$. Sometimes it is convenient to choose a somewhat different parametrization for the complex constants $C_n(0)$ [22]:

$$C_n(0) = 2\eta_n \left[\frac{(\xi_1 - \xi_2)^2 + (\eta_1 + \eta_2)^2}{(\xi_1 - \xi_2)^2 + (\eta_1 - \eta_2)^2} \right]^{1/2} \times \exp[\vartheta_n^0 + i\sigma_n^0 + i\varphi_n], \quad n = 1,2, \tag{A4}$$

where

$$\varphi_n = \pi/2 - \arctan\left[\frac{(\xi_n - \xi_{\tilde{n}})^2 + (\eta_n^2 - \eta_{\tilde{n}}^2)}{2\eta_{\tilde{n}}(\xi_n - \xi_{\tilde{n}})} \right], \quad n = 1,2,$$

and $\tilde{n} = 3 - n$. Instead of each complex constant $C_n(0)$ we have introduced two real constants ϑ_n^0 and σ_n^0 which are related to the initial position and phase of each soliton. A simple, though tedious, calculation yields the determinant of system (A2):

$$\det(\boldsymbol{I}+\boldsymbol{M}\boldsymbol{M}^{*}) = 2\exp[-2(\eta_1+\eta_2)t+\vartheta_1+\vartheta_2]\Delta, \tag{A5}$$

where the quantity Δ is

$$\Delta = \Delta(z,t) = \cosh[2(\eta_1+\eta_2)t-\vartheta_1-\vartheta_2] + \frac{4\eta_1\eta_2}{(\xi_1-\xi_2)^2+(\eta_1-\eta_2)^2}\cos[2(\xi_1-\xi_2)t+\sigma_1-\sigma_2] + \frac{(\xi_1-\xi_2)^2+(\eta_1+\eta_2)^2}{(\xi_1-\xi_2)^2+(\eta_1-\eta_2)^2}\cosh[2(\eta_1-\eta_2)t-(\vartheta_1-\vartheta_2)]. \tag{A6}$$

In Eq. (A6) the dynamics of the position ϑ and phase σ parameters of individual solitons is given by the expressions

$$\vartheta_n(z) = \vartheta_n^0 - 4\xi_n\eta_n z, \tag{A7}$$

$$\sigma_n(z) = \sigma_n^0 + 2(\xi_n^2-\eta_n^2)z. \tag{A8}$$

The explicit form for the Jost functions, parametrized through the amplitudes, velocities, phases, and positions, now is

$$\psi_1(z,t;\zeta_n) = \frac{i}{2\Delta}\sqrt{\frac{(\eta_n+\eta_{\tilde{n}})^2+(\xi_n-\xi_{\tilde{n}})^2}{(\eta_n-\eta_{\tilde{n}})^2+(\xi_n-\xi_{\tilde{n}})^2}}e^{-\eta_n t-i\xi_n t-i(\sigma_n+\varphi_n)}\left\{\frac{[\eta_n-\eta_{\tilde{n}}+i(\xi_n-\xi_{\tilde{n}})][\eta_n+\eta_{\tilde{n}}-i(\xi_n-\xi_{\tilde{n}})]}{(\eta_n+\eta_{\tilde{n}})^2+(\xi_n-\xi_{\tilde{n}})^2}e^{-2\eta_{\tilde{n}}t+\vartheta_{\tilde{n}}}+e^{2\eta_{\tilde{n}}t-\vartheta_{\tilde{n}}} + \frac{2\eta_{\tilde{n}}[\eta_n+\eta_{\tilde{n}}-i(\xi_n-\xi_{\tilde{n}})]}{(\eta_n+\eta_{\tilde{n}})^2+(\xi_n-\xi_{\tilde{n}})^2}e^{2\eta_n t-\vartheta_n+2i(\xi_n-\xi_{\tilde{n}})t+i(\sigma_n-\sigma_{\tilde{n}})}\right\}, \tag{A9}$$

$$\psi_2(z,t;\zeta_n) = \frac{1}{2\Delta}e^{\eta_n t+i\xi_n t-\theta_n}\left\{\frac{2\eta_{\tilde{n}}}{\eta_n-\eta_{\tilde{n}}+i(\xi_n-\xi_{\tilde{n}})}e^{-2\eta_n t+\vartheta_n-2i(\xi_n-\xi_{\tilde{n}})t-i(\sigma_n-\sigma_{\tilde{n}})}+\frac{\eta_n+\eta_{\tilde{n}}+i(\xi_n-\xi_{\tilde{n}})}{\eta_n-\eta_{\tilde{n}}+i(\xi_n-\xi_{\tilde{n}})}e^{-2\eta_{\tilde{n}}t+\vartheta_{\tilde{n}}}+e^{2\eta_{\tilde{n}}t-\vartheta_{\tilde{n}}}\right\}. \tag{A10}$$

Using these expressions from Eq. (A3) the general two-soliton solution can be written as [22]

$$q(z,t) = -\frac{2}{\Delta}\left(\frac{(\xi_1-\xi_2)^2+(\eta_1+\eta_2)^2}{(\xi_1-\xi_2)^2+(\eta_1-\eta_2)^2}\right)^{1/2}\{2\eta_1\cosh(2\eta_2 t-\vartheta_2-i\varphi_1)e^{-2i\xi_1 t-i\sigma_1}+2\eta_2\cosh(2\eta_1 t-\vartheta_1-i\varphi_2)e^{-2i\xi_2 t-i\sigma_2}\}. \tag{A11}$$

When the velocities are zero, $\xi_1=\xi_2=0$, the solution is a two-soliton breather representing a beating between the two periodically overlapping solitons. The overlapping occurs when the denominator $\Delta(z,t)$ at the origin $t=0$ takes its minimum value.

[1] Y. Kivshar and G. Agrawal, *Optical Solitons: From Fibers to Photonic Crystals* (Academic Press, San Diego, 2003); G. Agrawal, *Nonlinear Fiber Optics* (Academic Press, San Diego, 2001).

[2] A. Hasegawa and Y. Kodama, *Solitons in Optical Communications* (Clarendon Press, Oxford, 1995).

[3] V. E. Zakharov and A. B. Shabat, Zh. Eksp. Teor. Fiz. **61**, 118 (1971); [Sov. Phys. JETP **34**, 62 (1971)].

[4] S. V. Manakov, S. P. Novikov, L. P. Pitaevskii, and V. E. Zakharov, *Theory of Solitons* (Consultants Bureau, New York, 1984).

[5] N. R. Pereira and F. Y. F. Chu, Phys. Fluids **22**, 874 (1979).

[6] B. A. Malomed, Physica D **15**, 374 (1985); **15**, 385 (1985).

[7] K. J. Blow and N. J. Doran, Opt. Commun. **52**, 367 (1985).

[8] E. M. Dianov, Z. S. Nikonova, and V. N. Serkin, Kvantovaya Elektron. (Kiev) **13**, 331 (1986); [Sov. J. Quantum Electron. **16**, 219 (1986)].

[9] A. Hasegawa and T. Nyu, J. Lightwave Technol. **11**, 395 (1993).

[10] E. A. Golovchenko, E. M. Dianov, A. M. Prokhorov, and V. N. Serkin, Zh. Eksp. Teor. Fiz. **42**, 74 (1985); [JETP Lett. **42**, 87 (1985)].

[11] M. Gölles, I. M. Uzunov, and F. Lederer, Phys. Lett. A **231**, 195 (1997).

[12] Y. Kodama and K. Nozaki, Opt. Lett. **12**, 1038 (1987).

[13] K. S. Lee and J. A. Buck, J. Opt. Soc. Am. B **20**, 514 (2003).

[14] V. V. Afanasjev, J. S. Aitchison, and Y. S. Kivshar, Opt. Commun. **116**, 331 (1995).

[15] V. A. Aleshkevich, Y. V. Kartashov, A. S. Zelenina, V. A. Vysloukh, J. P. Torres, and L. Torner, Opt. Lett. **29**, 483 (2004).

[16] Y. V. Kartashov, L. C. Crasovan, A. S. Zelenina, V. A. Vysloukh, A. Sanpera, M. Lewenstein, and L. Torner, Phys. Rev. Lett. **93**, 143902 (2004).

[17] A. Suryato and E. van Groesen, Opt. Commun. **258**, 264 (2006).

[18] B. A. Malomed, Phys. Rev. A **44**, 6954 (1991).

[19] K. J. Blow, N. J. Doran, and D. Wood, Opt. Lett. **12**, 1011 (1987).

[20] V. V. Afanasjev, Opt. Lett. **18**, 790 (1993).
[21] Y. Kodama and S. Wabnitz, Opt. Lett. **16**, 1311 (1993).
[22] T. Okamawari, A. Hasegawa, and Y. Kodama, Phys. Rev. A **51**, 3203 (1995).
[23] T. Yamada and K. Nozaki, J. Phys. Soc. Jpn. **58**, 1944 (1989).
[24] S. Burtsev, R. Camassa, and I. Timofeyev, J. Comput. Phys. **147**, 166 (1998); G. Boffetta and A. R. Osborne, *ibid.* **102**, 252 (1992).
[25] V. V. Afanasjev, V. N. Serkin, and V. A. Vysloukh, Sov. Lightwave Commun. **2**, 35 (1992).
[26] D. J. Kaup, SIAM J. Appl. Math. **31**, 121 (1976); V. I. Karpman and E. M. Maslov, Zh. Eksp. Teor. Fiz. **73**, 537 (1977); [Sov. Phys. JETP **46**, 281 (1977)]; D. J. Kaup and A. C. Newell, Proc. R. Soc. London, Ser. A **361**, 413 (1978).
[27] V. I. Karpman and V. V. Solov'ev, Physica D **3**, 142 (1981); J. P. Gordon, Opt. Lett. **8**, 596 (1983).
[28] J. Satsuma and N. Yajima, Suppl. Prog. Theor. Phys. **55**, 284 (1974).